J. Mt. Sci. (2021) 18(1): 1-20 e-mail: jms@imde.ac.cn http://jms.imde.ac.cn
https://doi.org/10.1007/s11629-020-6552-y

Original Article

Field testing innovative differential geospatial and photogrammetric monitoring technologies in mountainous terrain near Ashcroft, British Columbia, Canada

David HUNTLEY[1*] https://orcid.org/0000-0002-9028-8022; e-mail: david.huntley@canada.ca

Peter BOBROWSKY[2#] https://orcid.org/0000-0001-7926-7776; e-mail: peter.bobrowsky@canada.ca

Roger MACLEOD[2] https://orcid.org/0000-0003-1714-8995; e-mail: roger.macleod@canada.ca

Robert COCKING[1] https://orcid.org/0000-0001-8952-7367; e-mail: robert.cocking@canada.ca

Jamel JOSEPH[1] https://orcid.org/0000-0003-2434-8151; e-mail: jamel.joseph@canada.ca

Drew ROTHERAM-CLARKE[1] https://orcid.org/0000-0002-8488-9489; e-mail: drew.rotheram-clarke@canada.ca

** Corresponding author; # Emeritus scientist*

1 Geological Survey of Canada, 1500-605 Robson Street, Vancouver, British Columbia,V6B 5J3, Canada

2 Geological Survey of Canada, 9860 West Saanich Road, Sidney, British Columbia, V8L 4B2, Canada

Citation: Huntley D, Bobrowsky P, Macleod R, et al. (2021) Field testing innovative differential geospatial and photogrammetric monitoring technologies in mountainous terrain near Ashcroft, British Columbia, Canada. Journal of Mountain Science 18(1). https://doi.org/10.1007/s11629-020-6552-y

© Science Press, Institute of Mountain Hazards and Environment, CAS and Springer-Verlag GmbH Germany, part of Springer Nature 2021

Abstract: This paper presents a novel approach to continuously monitor very slow-moving translational landslides in mountainous terrain using conventional and experimental differential global navigation satellite system (d-GNSS) technologies. A key research question addressed is whether displacement trends captured by a radio-frequency "mobile" d-GNSS network compare with the spatial and temporal patterns in activity indicated by satellite interferometric synthetic aperture radar (InSAR) and unmanned aerial vehicle (UAV) photogrammetry. Field testing undertaken at Ripley Landslide, near Ashcroft in south-central British Columbia, Canada, demonstrates the applicability of new geospatial technologies to monitoring ground control points (GCPs) and railway infrastructure on a landslide with small and slow annual displacements (<10 cm/yr). Each technique records increased landslide activity and ground displacement in late winter and early spring. During this interval, river and groundwater levels are at their lowest levels, while ground saturation rapidly increases in response to the thawing of surficial earth materials, and the infiltration of snowmelt and runoff occurs by way of deep-penetrating tension cracks at the head scarp and across the main slide body. Research over the last decade provides vital information for government agencies, national railway companies, and other stakeholders to understand geohazard risk, predict landslide movement, improve the safety, security, and resilience of Canada's transportation infrastructure; and reduce risks to the economy, environment, natural resources, and public safety.

Keywords: Landslide; Change detection monitoring; Global Navigation Satellite System; Real-Time Kinematic System; Geocube™; Bathymetric Survey; Unmanned Aerial Vehicle; Interferometric Synthetic Aperture Radar

Received: 03-Nov-2020
Accepted: 08-Dec-2020

1 Introduction

Global socioeconomic recovery and rehabilitation following the covid-19 pandemic will be strongly reliant upon transportation networks that are resilient to the adverse impacts of climate change and weather-driven geohazards (e.g., landslides, avalanches, floods and wildfires). For many countries, their national railway network will be the dominant mode for transporting natural resources to, and from coastal ports; and commuters and tourists to and from urban centres (Renner and Gardner 2010; Newman et al. 2013; Skrucany et al. 2017). Resilient railway transportation networks require sustainable, cost-effective management of service operations to meet future socioeconomic needs, and ensure protection of the natural environment (Jespersen-Groth et al. 2009; Laimer 2017; Aydin et al. 2018; Yang et al. 2019).

Where transportation corridors traverse unstable mountainous terrain, critical rail infrastructure is at risk of damage, and presents potential local and national economic, social, and environmental challenges (Schuster and Fleming 1986; Geertsema et al. 2009; Petrova 2011; Sun et al. 2013; Haque et al. 2016). The economic importance of these corridors, along with the need to understand and manage the safety risks related to landslides make on-site investigations a strategic priority for governments, the rail industry, and academia (Baum et al. 2005; Jaiswal et al. 2010; Doll et al. 2014; Martinović et al. 2016). Monitoring unstable slopes and infrastructure at risk is a cost-effective hazard management practice that also provides important geoscience information to help develop appropriate mitigation and adaptation measures (Ko Ko et al. 2005; Lindgren et al. 2009; Ronchetti et al. 2009; Gibson et al. 2012; Sa'adin et al. 2016).

In Canada, a safe and secure national rail network is essential for exporting natural resources (e.g., coal, oil, grain, potash, forest products) to deep-water marine terminals, and for goods entering continental North America from global markets. Unfortunately, across much of the country, vital railway infrastructure and operations are confined to transportation corridors where steep terrain is highly susceptible to landslide activity (Bobrowsky and Dominguez 2012). For both Canadian National (CN) and Canadian Pacific (CP) railways, tracks and infrastructure along the Thompson River valley between the communities of Ashcroft, Spences Bridge, and Lytton in southern British Columbia (Fig. 1a) are particularly vulnerable to landslides (VanDine 1983; Bobrowsky et al. 2014; Bobrowsky et al. 2017; Bobrowsky et al. 2018). Given the socio-economic importance of this transportation corridor, it is a priority for the Federal Government and Railway Industry to understand and manage the safety risk related to landslides that threaten this vital route. Monitoring and early warning for maintenance, and cautionary speed enforcement are considered the most effective strategies for management of risk given the economic costs and environmental consequences of attempting to stabilize slopes along the transportation corridor (Bunce and Chadwick 2012).

In this paper, we compare and evaluate the agreement and reliability of ground motion measurements from several complimentary landscape monitoring technologies under harsh environmental conditions at Ripley Landslide, located near Ashcroft in south-central British Columbia (Fig. 1b; Fig. 2). This includes real-time kinematic (RTK) global navigation satellite system (GNSS) surveys, continuous monitoring multi-frequency GNSS stations, and a network of single frequency differential (d-) GNSS sensors (Geocubes™). Additionally, we compare these measurements with displacements obtained from persistent scatterer (PS) interferometric synthetic aperture radar (InSAR) results, and structure from motion (SfM) analysis using imagery acquired from an unmanned aerial vehicle (UAV). Combined, these technologies provide contextual information understanding the influence of surficial geology and internal structure of monitored slopes, and external climate-driven variables (e.g., air temperature, precipitation, river level, groundwater levels) on landslide activity.

2 Landslide Research and Monitoring in the Thompson River Valley

Landslides along the ten kilometre stretch of the Thompson River valley south of Ashcroft (Fig. 1b) have impacted critical railway infrastructure, arable land, fisheries, and other natural resources since the 1880s (Stanton 1898; Clague and Evans 2003). Although some landslides failed and moved rapidly in the past, today all are slow-moving reactivated compound features within Pleistocene valley fill.

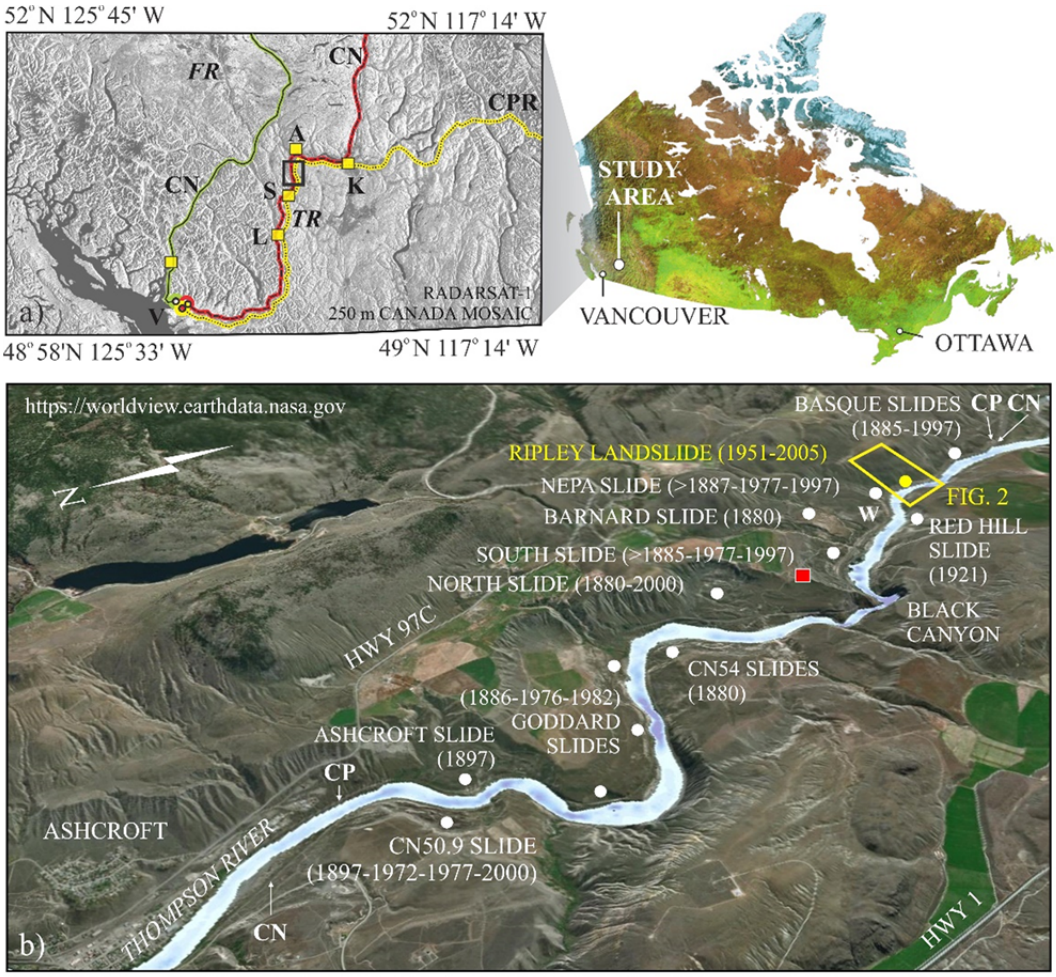

Fig. 1 The study area. a) Rail transportation corridors in southwestern British Columbia with location of the Thompson River valley area of interest (black rectangle): A – Ashcroft; K – Kamloops; L – Lytton; S – Spences Bridge; V – Vancouver; FR – Fraser River; TR - Thompson River. b) Landslide history of the Thompson River valley, showing location of Ashcroft and railway transportation corridor in relation to the Ripley Landslide test site (yellow text and dot); prime ground control point, survey base station (red square); weather station (W).

Glaciolacustrine clay-silt units, overlain by subglacial till diamictons, proglacial sand and gravel outwash, and alluvial fans with interbedded silt sand and debris flow diamictons, are significant hydrogeological controls on the distribution, geometry, and rate of landslide activity in the valley (Porter et al. 2002Eshraghian et al. 2007; Eshraghian et al. 2007; Bunce and Chadwick 2012; Huntley et al. 2020a).

Large rotational and retrogressive translational landslides were initially triggered by deep incision of Pleistocene fill in the Thompson River valley during the early Holocene (Clague and Evans 2003; Eshraghian et al. 2007; Eshraghian et al. 2008). Subsequently, Thompson River has influenced landslide stability by changing: 1) the pore water pressure in the slope mass, and in particular along rupture surfaces; 2) the supporting force on landslide toes; and, 3) through cutbank erosion, thereby affecting the geometry of the landslide. For most landslides, movement occurs along weak, sub-horizontal glaciolacustrine clay-silt rupture zones confined between overlying till and underlying bedrock. This movement is accommodated by one or more of three failure mechanisms: 1) slow-moving (2 cm to 10 cm/yr) rotational failures with large back-tilted blocks; 2) slow-moving (2 cm to 10 cm/yr) retrogressive translational slides with little rotation; and 3) rapid debris slumps involving flowage and sliding of landslide material (Porter et al. 2002; Clague and Evans 2003; Eshraghian et al. 2007; Eshraghian et al. 2008). Possible anthropogenic triggers include the irrigation of glacial terraces beginning in the 1860s, and the excavation of lower landslide slopes during the construction and

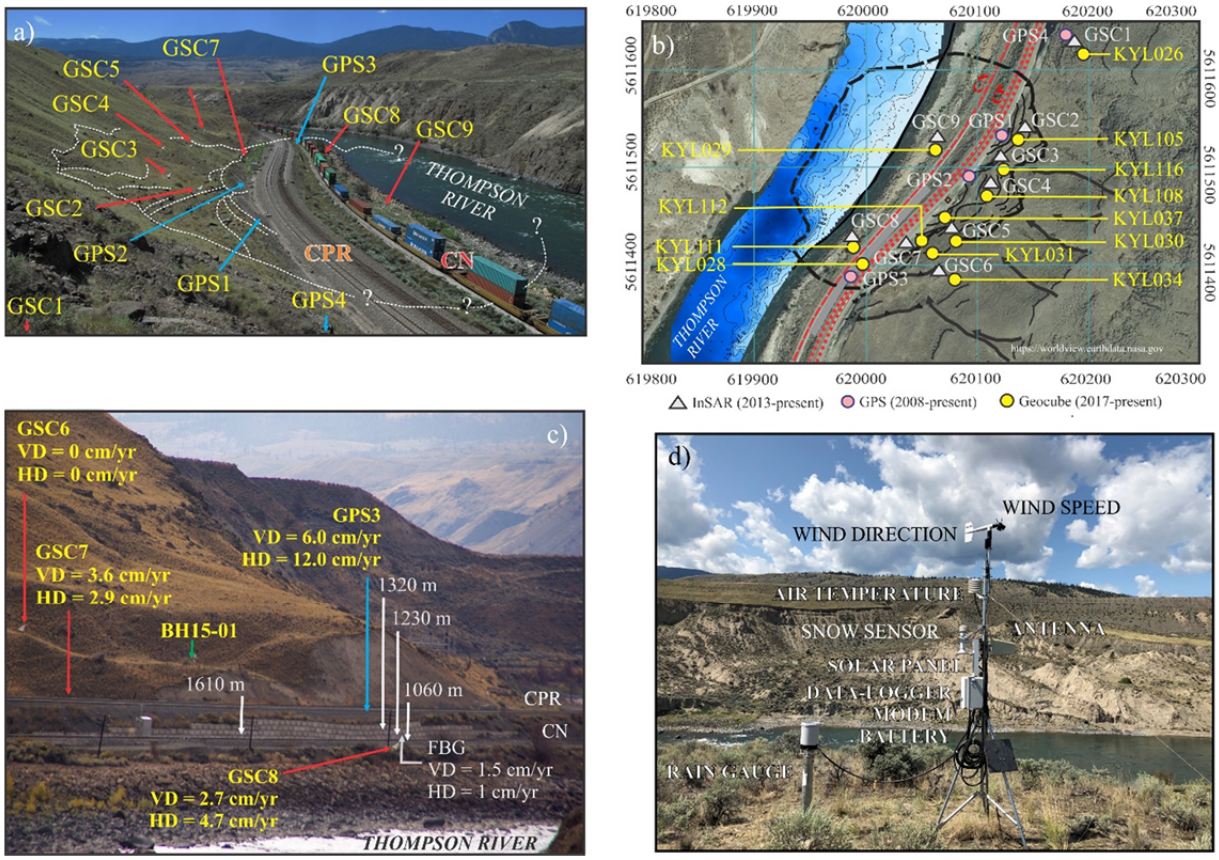

Fig. 2 a) Overview of the test site highlighting the location of GNSS monitoring stations (GPS1-4), InSAR corner reflectors (GSC1-9), and the monitored retaining wall dividing the CN and CPR tracks - view to south (Natural Resources Canada [NRCAN] Photo 2020-836). b) Plan view of the test site highlighting the location of GNSS monitoring stations (GPS1-4), InSAR corner reflectors (GSC1-9) and Geocubes™ (KYL026-KYL116). Railway infrastructure: CN track - red dashed line; CP tracks – red dotted lines; monitored lock-block retaining wall dividing the CN and CPR tracks - light grey solid line. Bathymetry derived from GPR and single-beam acoustic depth soundings (modified from Huntley et al. 2017a). c) South flank of landslide with sagging retaining wall separating CN and CPR tracks with displacement vectors for FBG, GNSS and InSAR stations; strain points detected by BOTDR (white arrows and distance in metres from datum); VD – vertical displacement; HD – horizontal displacement detected by FBG (grey arrow with displacement values expressed as mm/yr); and location of BH15-01 (green arrow) (NRCAN Photo 2020-837). d) Weather station installed in 2016, and continuously recording climate variables since (for location, see Fig 1b) (NRCAN Photo 2020-838).

expansion of the right-of-way for CP and CN tracks in the late 1800s and early 1900s (Stanton 1898; Clague and Evans 2003).

The Geological Survey of Canada (GSC), in collaboration with international and national partners of the Transport Canada (TC) Railway Ground Hazard Research Program (RGHRP), is assessing innovative methods for monitoring landslides in the Thompson River valley (Fig. 1b). As part of the International Consortium on Landslides (ICL) International Programme on Landslides (IPL) Project 202, landslides in the valley serve as field laboratories to test and compare the reliability and effectiveness of different static, dynamic, and real-time monitoring technologies (e.g., Huntley and Bobrowsky 2014; Huntley et al. 2016; Huntley et al. 2017a, b).

2.1 Ripley landslide test site

Ripley Landslide, located 7 km south of Ashcroft (Fig. 1 b), is approximately 220 m wide (N-S) by 150 m long (E-W), with an estimated volume of 400,000 m³ (Fig. 2 a, b). At the test site, valley fill consists of a wide range of sediments reflecting variability in the nature of their depositional environments over at least one glacial cycle during the Pleistocene Epoch (Huntley and Bobrowsky 2014; Huntley et al. 2020a). Similar to other landslides in the Thompson River valley, the landslide displays a retrogressive behaviour, with translational failure occurring along

sub-horizontal or listric rupture surfaces in weak, glacially sheared clay-rich rupture zones (Macciotta et al. 2014; Hendry et al. 2015; Schafer et al. 2015; Huntley et al. 2019a, b; Holmes et al. 2020).

An ancient landslide was reactivated in the early 1950s, and after 2005 following track maintenance, construction of embankments, and installation slope buttressing infrastructure across its central portion (Bunce and Chadwick 2012). Pronounced sagging and bulging of the lock-block retaining wall separating the CN and CP tracks has occurred since 2005 (Huntley et al. 2016; Huntley 2017 b, c). To accommodate continual lateral and vertical displacement across the landslide and minimize service disruption, both rail companies monitor track conditions, and must periodically add ballast to lift and re-aligning their rails and ties.

Numerous conventional and experimental continuous monitoring technologies provide insight on the activity, deformation mechanisms, and potential acceleration triggers of Ripley Landslide (Bunce and Chadwick 2012; Journault et al. 2018; Huntley et al. 2019a, b, c). Subsurface borehole monitoring combining ShapeAccelArray inclinometry with piezometer head levels indicate that the main slide body is failing along sub-horizontal, weak, basal shear surfaces in highly plastic clay beds (Macciotta et al. 2014; Hendry et al. 2015; Schafer et al. 2015). The central and northern parts of the landslide are translating sub-horizontally (2.1° to 2.5°), whereas the southern portion near the lock-block retaining wall has a steeper (28°) slide surface. Fibre Bragg grating (FBG) and Brillouin optical time domain reflectometry (BOTDR) monitoring of the retaining wall from 2013 to 2015 detected ~0.2 cm of accumulated strain in the wall. This strain contributed to 0.15 cm/yr vertical displacement and 0.1 cm/yr horizontal displacement of individual blocks at the southern end of the retaining wall, with peak activity occurring in the fall and winter months (Huntley et al. 2016; 2017c, d).

InSAR change detection monitoring using imagery acquired by Canada's RADARSAT-2 has been ongoing since 2013 (Huntley et al. 2017b; Journault et al. 2018). To define magnitudes and spatial-temporal patterns of surface displacement, three ultra-fine microwave beam modes (3 m spatial resolution) are used in the descending orbital node: U5 with an incident angle 34° and azimuth line-of-sight (LoS) of 281°; U16 incident angle 42°, azimuth LoS ≈280°; and U21 with a 45° incident angle and azimuth LoS of 279°. Aluminum trihedral (corner) reflectors are installed at Ripley Landslide for coherent point analysis of persistent scatterer interferograms. Corner reflectors GSC1 and GSC6 rest on stable ground – bedrock and till respectively; GSC2 to GSC5 and GSC7 to GSC9 are installed on unstable terrain (Fig. 2a). Different viewing geometries allow for the projection of vertical and horizontal displacement (Table 1).

Ground movement is concentrated within the main body of the sliding mass and averages 6 cm/yr, with fastest displacements detected upslope of the railway tracks (Fig. 3a). For May 2014 to April 2016, non-linear behavior can be sub-divided into 5 periods (Table 1). Rates of displacement detected by InSAR vary seasonally, with slower displacement rates occurring during the May to August interval, and higher values from September to April. Almost no vertical displacement was detected during May to August 2014 (Huntley et al. 2017c). In 2017, LoS displacement rate of coherent targets (e.g., corner reflectors, buildings, large boulders), equivalent to the downslope direction for the west-facing test site, was >10 cm/yr (Fig. 3b; A. Pon, pers. comm. 2019).

Table 1 Two-dimensional line-of-sight (LoS) displacement rates (cm/yr) for trihedral corner reflectors installed at Ripley Landslide. P1 - August 2013 to April 2014; P2 - May 2014 to August 2014; P3 - September 2014 to April 2015; P4 - May 2015 to August 2015; P5 -September 2015 to April 2016 (adapted from: Huntley et al. 2017b).

InSAR reflector	Vertical (cm/yr)				Horizontal Azimuth 280° (cm/yr)			
	Average	P1	P2-P3	P4-P5	Average	P1	P2-P3	P4-P5
GSC1	0	0	0	-1	0	0	0	0
GSC2	-3.0	-1.8	-0.8	-2.9	-4.1	-11.0	-4.6	-4.3
GSC3	-2.5	-0.9	-0.3	-2.6	-3.7	-11.1	-4.4	-3.5
GSC4	-2.2	-0.6	-0.2	-2.8	-3.2	-10.1	-4.0	-2.8
GSC5	-3.3	-4.9	-0.6	-2.6	-1.8	-5.6	-3.4	-2.1
GSC6	0	0	0	0	0	0	0	0
GSC7	-3.6	-7.8	-0.5	-2.4	-2.9	-5.0	-5.6	-2.9
GSC8	-2.7	-3.1	-0.4	-1.3	-4.7	-12.0	-6.3	-5.1
GSC9	-2.3	-2.7	-1.9	-2.5	-4.7	-16.2	-3.6	-4.5

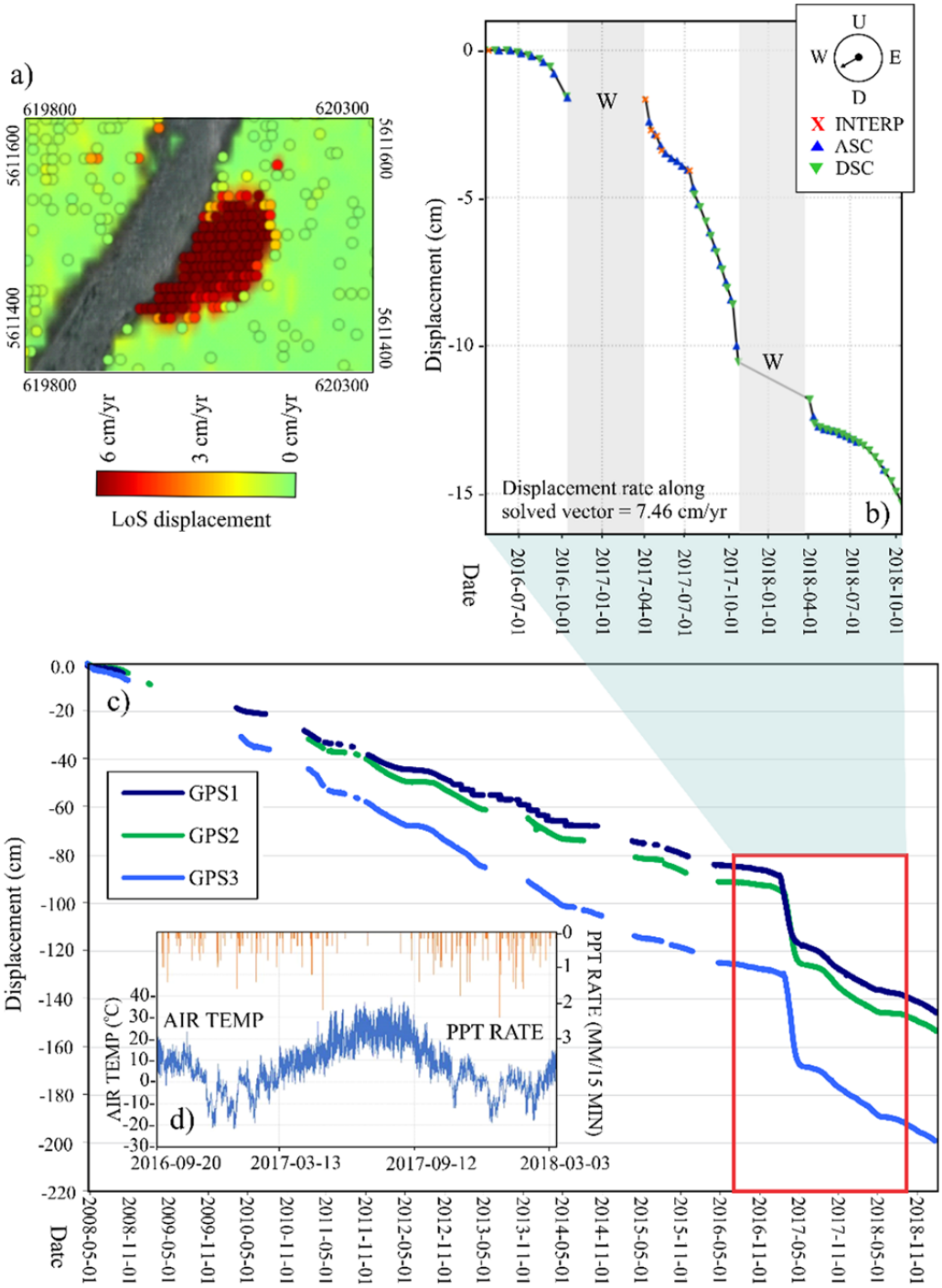

Fig. 3 Long term change detection monitoring at Ripley Landslide: a, b) InSAR average and 1D line-of-sight (LoS) displacement rates calculated using temporary coherent targets identified across RADARSAT-2 scenes from July 2016 to October 2018. Multi-master interferograms were created (minus winter scenes, W) with atmospheric effects removed, and signal enhancement including pixel searching and adaptive filtering (data and imagery courtesy of A. Pon, 3vGeomatics). c) Vertical displacement (cm) trackside from May 2008 to January 2019 recorded by GPS1 (-145 cm), GPS2 (-155 cm) and GPS3 (-200 cm); see Fig. 2 for location of GNSS monuments (GNSS data courtesy of D. Wong, CP). d) Air temperature and precipitation rate recorded at Thompson Valley weather station.

Four permanent GNSS monuments installed trackside across the landslide in 2008 (Fig. 2) record cumulative annual displacements >1.0 cm/yr to <6.0 cm/yr, with peak movement in winter (Bunce and Chadwick 2012; Macciotta et al. 2014; Hendry et al. 2015). GNSS monuments captured the 2017

displacement event, recording 4.7 cm/yr at the north end of the slide, and 5.2 cm/yr on the lock-block retaining wall (Fig. 3c). Two areas of maximum displacement recorded by these GNSS stations coincide with maximum displacement indicated by the corner reflectors (Table 1). The larger zone spans the CN and CP tracks between GSC3 to GSC5, GPS1 and GPS2, and GSC9. A smaller zone is centred on GSC7, GPS3 and GSC8 at the south end of the landslide near the lock-block retaining wall (Fig. 2).

At Ripley Landslide, peak creep rates are observed through winter to spring, indicating that river and groundwater levels do not account for all movement. During the 2016 field season, a total weather station was installed in the Thompson River valley to test whether a component of landslide movement can be attributed to local weather conditions; in particular, precipitation and temperature (Fig. 2b). The 18-month climate record (Fig. 3d) spanning a large displacement event shows that precipitation events were confined mostly between fall and spring, during months when landslide activity increases. Fluctuations in temperature over the winter months may contribute to intervals of landslide activity (Huntley et al. 2019c; Holmes et al. 2020).

2.2 Knowledge gap and monitoring limitations

A critical knowledge gap for landslide warning, forecasting, and risk reduction is the poorly defined spatial and temporal distribution of movement/ displacement across the unstable slope from year to year. At Ripley Landslide, interferometric analysis of RADARSAT-2 imagery provides spatially expansive records of motion of the slide body, but has low accuracy, is restricted to line-of-sight components, and observation intervals are limited by orbital paths. GNSS systems capture three-dimensional displacement vectors with high temporal resolution, and so complement remote sensing techniques by providing baseline surface mapping datasets and measures of landslide activity (e.g., Gili et al. 2000; Malet et al. 2002; Benoit et al. 2017; Raso et al. 2017; Macciotta et al. 2017; Rodriguez et al. 2018). Permanent GNSS monuments record time-referenced coordinates that precisely characterize the timing, rate, and direction of movement at three trackside locations (Fig. 2; Fig. 3b).

3 Methods of Investigation

3.1 Approach to study

Effective near real-time warning and forecasting of landslide activity (e.g., rate of movement, cumulative displacement, annual displacement) require "ruggedized" monitoring systems with sub-metre accuracy positioning in three dimensions; and monthly, diurnal, or hourly temporal resolution. Numerous studies have successfully employed GNSS techniques to determine the three-dimensional coordinates of moving points on landslides (Gili et al. 2000; Malet et al. 2002; Benoit et al. 2017; Macciotta et al. 2017; Raso et al. 2017; Rodriguez et al. 2018). However, periodic and continuous monitoring of ground control points (GCPs) and railway infrastructure with small and slow annual displacements (<10 cm/yr) is particularly challenging in an environment with a semi-arid intermontane climate, and an extreme temperature range of -30°C to +40°C. This section outlines the methods of change detection monitoring deployed at the test site to improve the spatial and temporal resolution of slope deformation.

3.2 Real-Time Kinetic GNSS surveying

The aim of repeat RTK-GNSS ground surveys was to better characterize the magnitude and direction of landslide movement over time. Rigorous change detection requires an accurate and precise elevation model to serve as a reference base map. In 2016, GCPs were established across the slope using stable boulders and anthropogenic features on, and adjacent to the landslide (Fig. 4). A reference base station was established on a stable post-glacial terrace near Black Canyon, 3 km north the Ripley Landslide (Fig. 1b). The absolute position of this prime GCP was determined from a post-processed RINEX file using the Canadian Spatial Reference System Precise Point Positioning tool after a nine-hour occupation. The reported absolute positional accuracy was 0.8 cm horizontally and 1.3 cm vertically (95% Σ), and these values were used for all surveys (Fig. 1b; Fig. 4a). RTK-GNSS rover measurements were occupied for a minimum of two minutes at 1 Hz, and reported a horizontal precision of better than 2 cm and a vertical precision of 3 cm. All RTK-GNSS positioning data were reviewed, corrected for antenna laybacks,

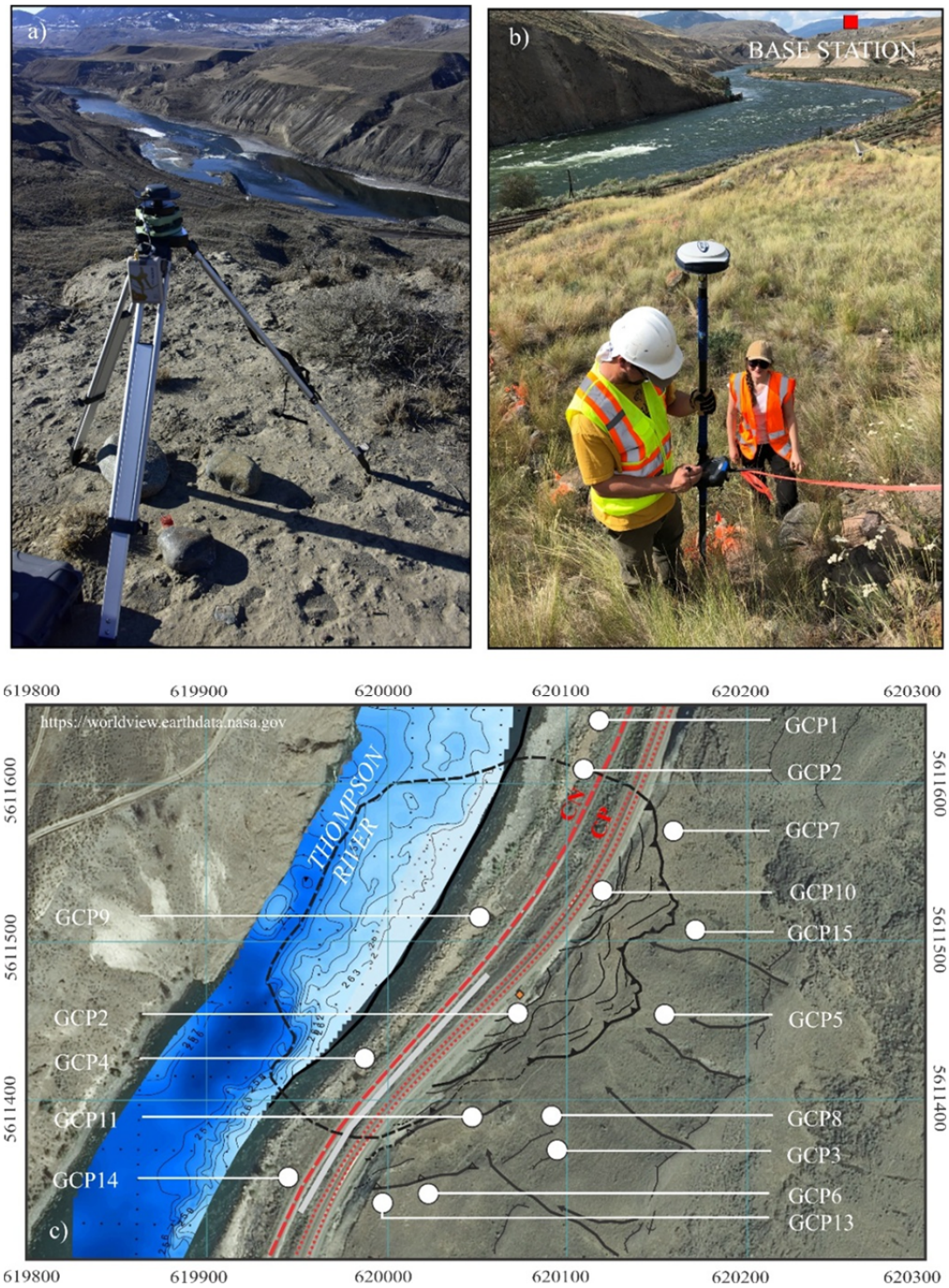

Fig. 4 a) Base station at South Slide, with EOS Arrow Gold base unit positioned over the prime GCP (March 2019) (NRCAN Photo 2020-839); b) Trimble Spectra SP-80 RTK GNSS head and Spectra TSC3 Ranger handheld computer (NRCAN Photo 2020-840); c) distribution of ground control points (GCPs) on and adjacent to Ripley Landslide.

heights and edited for erroneous data points during the data processing (Huntley et al. 2017a).

3.3 Bathymetric surveying

The aim of the bathymetric surveys was to better characterize the geometry of submerged landslide toe slopes, and identify reaches with channel incision and erosion. Between 2014 and 2018, bathymetric surveys were completed along a 10 km reach of Thompson River from Ashcroft to Basque Landslide using ground-penetrating radar (GPR) (Huntley et al. 2017a, b; Fig. 5a), a BioSonics® DTX single-beam hydro-acoustic echo sounder (Fig. 5b), and NORBIT wide

multi-beam integrated sonar (Fig. 5c). The GPR unit was mounted midship on a rubber raft (Fig. 5a), while the echo sounder and multi-beam sonar were mounted midship, or off the starboard side of the swim board at the stern of a 5 m-long aluminum-hulled jet boat (Fig. 5b, c). Each survey day, water level at the Ashcroft boat launch was measured using a RTK-GNSS rover. To provide high-precision data, boat speed was maintained between 5 km/hr and 8 km/hr for both the single-beam and multi-beam surveys. Depth data were collected by traversing the study reach at approximately 100 m intervals during single-beam surveys, and at a 10 m spacing between transect lines during multi-beam surveys. Cold temperatures and very low river levels over the winters of 2016-2017 and 2018-2019 produced operational safety concerns, limiting bathymetric surveys to the thalweg (i.e. the longitudinal path of greatest depth down the channel). Data acquisition was limited in shallow water or high velocity rapids. RTK-GNSS rovers were also used to measure water surface, wetted width, and bank elevations up to the high-water mark at channel gradient changes (e.g., upstream and downstream ends of rapids where data quality was poor or absent). Positional control for single-beam acoustic waterborne surveys was provided using the RTK-GNSS rovers and onboard GNSS receivers. The multi-beam system included a RTK-GNSS and an inertial navigation system to correct for attitude, heading, heave, position, and velocity. A water profile sensor was used to correct sound velocity in the water column. Post-processing, using Teledyne CARIS software, included filtering and merging of data using overlapping passes.

3.4 Differential GNSS monitoring with GeocubesTM

The aim of the differential (d-) GNSS monitoring was to was to better characterize the timing, rate, and direction of landslide movement across the landslide body. Repeat RTK-GNSS surveys provided point position data across much of the slide body. However, this method generated limited information on the seasonal variation in displacement rates and amounts. GNSS monuments (Bunce and Chadwick 2012; Macciotta et al. 2014) provide continuous, near-real-time monitoring of surface displacement, but only at three trackside locations (Fig. 2). Starting in 2016, a Geocube (GeoKylia)™ d-GNSS network was installed

Fig. 5 a) GPR survey of Thompson River at Ripley Landslide executed with GPR transmitter and receiver mounted on a river raft, towed by jet boat then released and steered while recording (November 2014) (NRCAN Photo 2020-841); b) BioSonics® DTX hydro-acoustic Echo Sounder mounted at the stern of the jet boat (NRCAN Photo 2020-842); c) NORBIT multi-beam system mounted broadside with GNSS antenna attached (NRCAN Photo 2020-843).

at Ripley Landslide to address both issues of spatial and temporal coverage (cf. Benoit et al. 2015; Macciotta et al. 2017; Raso et al. 2017; Rodriguez et al. 2018). This monitoring system comprised twelve small, rugged, single-frequency d-GNSS transmitter-receivers with directional radio communication

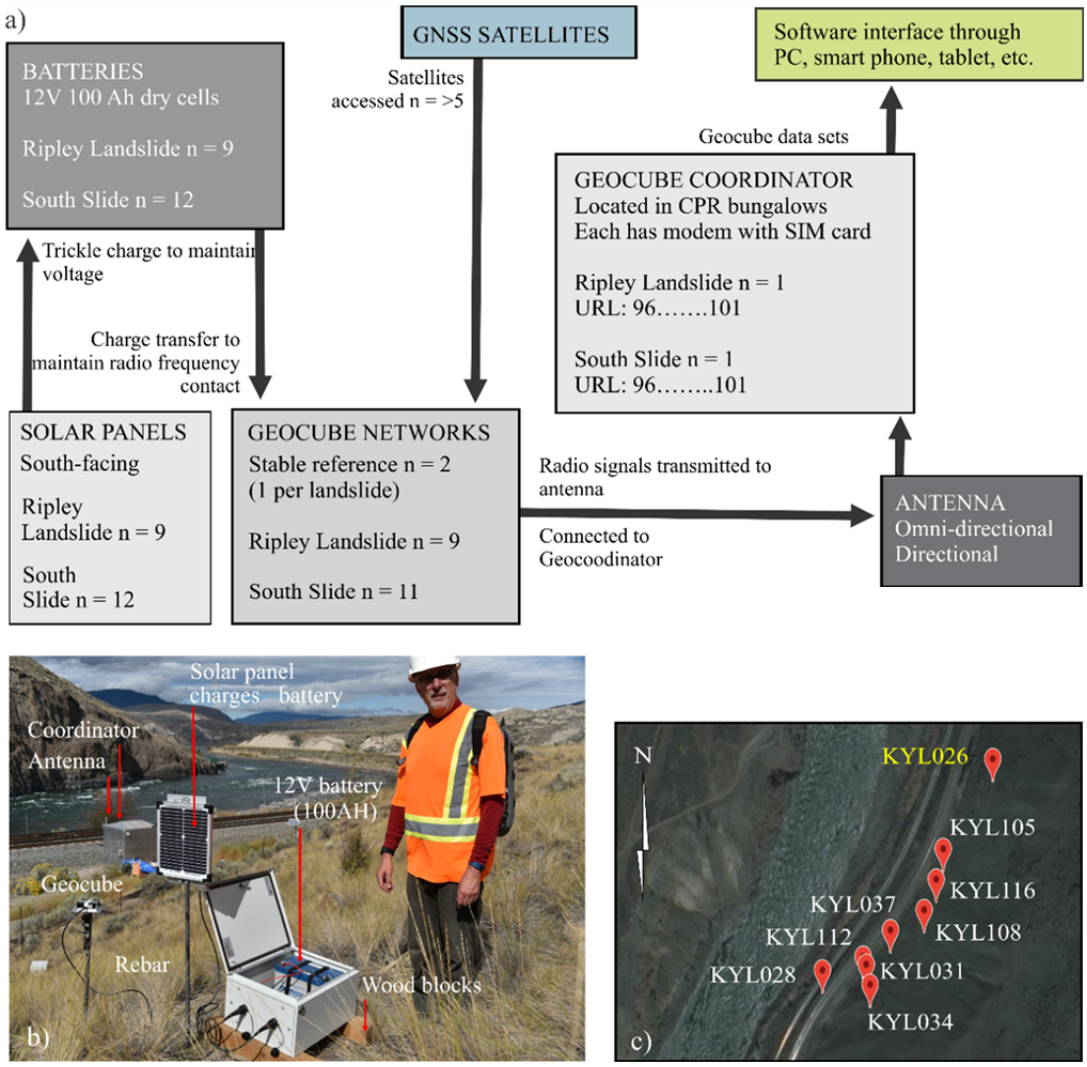

Fig. 6 Geocube™ d-GNSS installation: a) schematic of Geocube™ system (NRCAN Photo 2020-844); b) components installed on the unstable slope; c) Geocube™ network installed at Ripley Landslide (yellow text label is stable reference position).

antennas that relayed geospatial data to a coordinator unit hosting a proprietary operating system (Huntley et al. 2020b). A 3G network modem with an omnidirectional antenna provided internet access to the coordinator (Fig. 6a). These single frequency receivers recorded raw carrier phase data, and were corrected to the base station using short baselines. These two qualities allowed the network to achieve a precision of 2 to 5 mm horizontally, and 4 to 10 mm vertically (Benoit et al. 2015). For Ripley Landslide, d-GNSS units were positioned ensure units were able to receive satellite signals, while maintaining lines-of-sight with the antenna. Solar panels were positioned to maintain maximum exposure to the sun when oriented facing south (Fig. 6b). One d-GNSS unit was installed on stable terrain adjacent to stations GSC1 and GPS4: a bedrock outcrop that confined the landslide in the northeast (Fig. 2); the remaining eleven were positioned across the slide body to capture spatial variation in displacement (Fig. 6c). Along the railway right-of-way, signal transmissions between the d-GNSS units and coordinator were periodically blocked and reflected by rolling stock, active tracks, scrapped rail stockpiles, and the lock block retaining wall.

3.5 UAV surveying and change detection monitoring

Beginning in September 2016, repeat UAV surveys of Ripley Landslide have aimed to better characterize the spatial extent, magnitude and

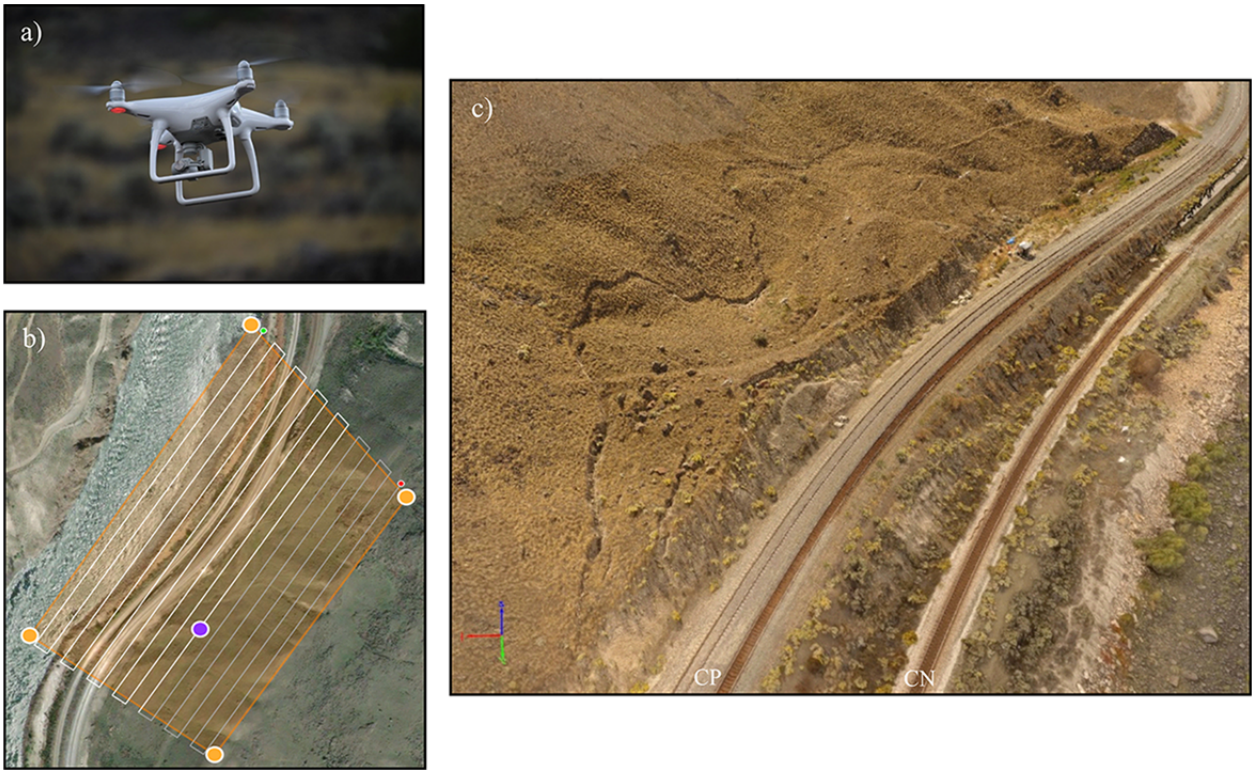

Fig. 7 a) DJI Phantom 4 UAV (NRCAN Photo 2020-845); b) Programmed flight plan for Ripley Landslide September 2019 survey (image: P. Skrivanos); c) DSM of landslide generated by SfM software (September 2016).

direction of landslide movement (Fig. 7a, b). UAVs allow flexible, inexpensive acquisition of low-altitude aerial imagery, while various off-the-shelf photogrammetric software packages enable production of high-resolution digital surface models (DSM) from such images. UAV survey flight planning was conducted using Pix4D Capture (2016, 2017) and Map Pilot (2018, 2019); the SfM modelling was undertaken using Pix4D Mapper. Plan-view and oblique colour aerial photographs were merged using SfM software, and DSMs then generated at a pixel resolution of 2 cm (Fig. 7c). Planimetric displacement of the landslide was first mapped using an ENVI 5.2 plug-in called Cosi-Corr (Co-registration of Optically sensed Images and Correlation) developed by the California Institute of Technology. Co-relation processing was conducted on hill-shaded UAV DSMs of the landslide with 1.5 times exaggeration, and the sun at azimuth 310° and 45° altitude. Areas of vegetation, and recent track ballast work on hill-shaded images were masked prior to co-relation processing to reduce the areas with substantial change not related to slide movement. Two images (September 2016 to September 2017, and September 2017 to October 2018) were created for E/W (X) and N/S (Y) displacement, while elevation changes (Z) were derived from the DSM. These values were then added and squared to produce a single raster containing 3D displacement values that were all positive (larger values = more displacement).

4 Results and Interpretations

4.1 Real-Time Kinetic GNSS surveying

A total of 15 GCPs are positioned on stable b oulders and anthropogenic features (Fig. 4c). Large changes in Z values (~15 m) between 2017, 2018 and 2019 surveys are related to a datum shift at the prime GCP (Fig 1b), and so have been excluded from further discussion. Five GCPs record significant horizontal displacement on the landslide (Table 2). Upslope of the train tracks, on the main slide body, GCP10 records 8.7 cm of movement to the NNW; and GCP12 captures 16.1 cm of NW displacement. Disturbance during track maintenance accounts for the anomalous vector for GCP10 and slower displacement rate. Downslope of the tracks across the slide toe, 11.3 cm of WNW displacement is measured at GCP02; GCP04

Table 2 Ground control points (GCPs) recording total horizontal displacement in centimetres (Δ N-Northing, ΔE-Easting) from September 2017 to September 2019.

UTM Zone 10	Northing	Easting	Northing	Easting
Survey date	GCP-02		GCP-04	
30/9/2017	620101.7468	5611603.802	619983.3499	5611431.344
30/6/2018	620101.7912	5611603.862	619983.2662	5611431.423
30/10/2018	620101.754	5611603.889	619983.238	5611431.433
15/08/2019	620101.716	5611603.892	619983.206	5611431.473
30/09/2019	620101.729	5611603.913	619983.192	5611431.483
Δ N / Δ E	1.7798 cm	-11.118 cm	15.7943 cm	-13.93 cm
Survey date	GCP-09			
30/9/2017	620045.3471	5611522.005		
30/6/2018	620045.3272	5611522.063		
30/10/2018	620045.278	5611522.085		
15/08/2019	620045.221	5611522.132		
30/09/2019	620045.23	5611522.145		
Δ N / Δ E	11.7065 cm	-14.018 cm		
Survey date	GCP-10		GCP-12	
30/9/2017	-	-	620072.3907	5611451.301
30/6/2018	620116.6772	5611533.564	620072.3152	5611451.367
30/10/2018	620116.651	5611533.579	620072.308	5611451.359
15/08/2019	620116.609	5611533.598	620072.262	5611451.398
30/09/2019	620116.595	5611533.59	620072.3907	5611451.301
Δ N / Δ E	8.2157 cm	-2.605 cm	12.8706 cm	-9.651 cm

is displaced 16.4 cm NW; and GCP09 moved 18.3 cm NW over the three year observation period. The remaining GCPs are on stable portions of the slope, and adjacent to the landslide (Fig. 4c).

4.2 Bathymetric surveying

Bathymetric maps of Thompson River and Ripley Landslide were created by post-processing and correction of raw single-beam and multi-beam survey data using EchoVIEW and Teledyne CARIS software, respectively. Bank and water surface elevation data were used to assist with tying bathymetric data into UAV DSMs. The November 2014, March 2015, October 2017, and November 2018 river surveys reveal variations in bed composition ranging from sand and silt draping bedrock, to coarse gravel and boulders overlying clay-rich valley fill. Shallow waters (riffles) with rapids lie adjacent to stable terrain, separated by deep scour pools (typically 5-10 m below river level) adjacent to the toes of all landslides (Fig. 1 b; Fig. 2 b).

With fast currents and white-water conditions, the jet boat is pitched, rolled, and yawed more than typical watercraft. Single-beam inertial measurement units are too slow to accurately record the rapid changes in attitude, for example the scour features at landslide toes (e.g. Ripley Landslide). Some scour pools (e.g. Black Canyon, >45 m) are too deep for strong single-beam acoustic signal returns. The multibeam system provides complete coverage, but only for the slide areas in deeper water (pools). Surveying is not possible in rapids and in shallow waters (i.e. riffles) where the sonar system is confused by air bubbles caused by the current and turbulent water. This produces a considerable noise requiring post-survey manual clean-up of data. Shallow water requires a large number of passes, increasing the likelihood of bottoming-out and damaging equipment.

4.3 Differential GNSS monitoring with GeocubesTM

Geocubes™ displacement results from November 2018 to June 2019 are discussed here. Eight d-GNSS units installed across Ripley Landslide were active to some degree, and recording 3D displacement during this time interval (Fig. 8). Three units were inactive due to wildlife damage or low battery charge (KYL029, KYL030, KYL111). Location data (X - longitude, Y - latitude, Z – height above sea level) collected over the eight month-long observation trial, imported into an ArcGIS Geodatabase, are plotted as points, grey-shaded from light to dark according to date (per month) (Fig. 8).

Immediately apparent is the generally NW displacement trend for all working d-GNSS units, with unfiltered data charting a helical drift over the months of observation (Fig. 9). The most reliable units (KYL105, KYL108, KYL112, and KYL116) are the

focus of discussion. Relative location data (X, Y, Z) averaged every 15 days over the eight month-long observation trial are plotted as points overlying precipitation and temperature data (Fig. 9). The NW displacement trends are consistent with the displacement vectors derived from change detection analysis of the RTK-GNSS survey, and UAV imagery using the SfM and Cosi-Corr software (Fig. 10).

In the northern sector of the landslide, d-GNSS units capture movement at varying rates from November 2018 to June 2019, suggesting displacement of multiple slide blocks along moderately steep-dipping backscarps. The unit on the most northerly block moved horizontally NW 5.55 cm, while dropping 1.8 cm in elevation (KYL105). A second unit, in a graben block, moved NW 4.5 cm with a 1.7 cm drop in elevation (KYL116). The third unit, on the central block, moved horizontally NW 5.0 cm, dropping 1.5 cm (KYL108) over the eight-month trial (Fig. 8; Fig. 9).

In the southern sector, generally slower horizontal, but greater vertical displacements are recorded over the eight month observation period. KYL037 captured 3.2 cm horizontal movement to the NW, with a drop of 3.0 cm on the slide block near the CP tracks and signals bungalow. Similar to KYL116 in the northern sector of the slide body, KYL031 and KYL112 are located in a graben toward the southern margin of the slide. KYL031 moved horizontally NW 0.1 cm prior to power failure during the winter. While experiencing only 3.4 cm of horizontal movement NW, KYL112 dropped 1.8 cm in elevation. On the lock-block retaining wall, KYL028 recorded 3.9 cm of horizontal movement NW, and experienced 3.2 cm vertical downward displacement - the greatest vertical downward displacement across the slide body – before power failure in early May 2019 (Fig. 8). Above the southern head scarp, KYL034 captured 1.2 cm of horizontal movement to W, while dropping in height by 0.08 cm. These small displacement values may be an indication of developing (i.e. retrogressive) instability upslope of the active headscarp.

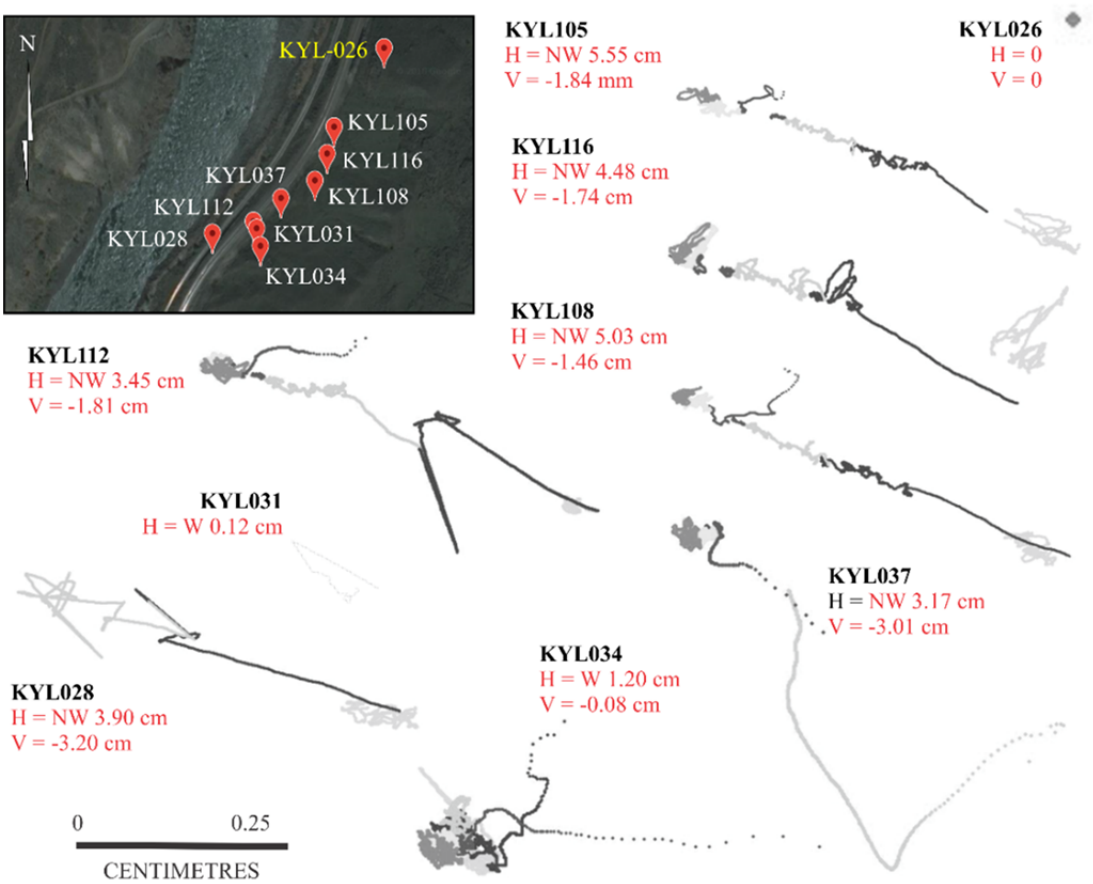

Fig. 8 a) Unfiltered displacement trends of Ripley Landslide Geocube™ d-GNSS network. Google Earth image showing active units from December 2018 and provisional results for the November 2018 to June 2019 observation period.

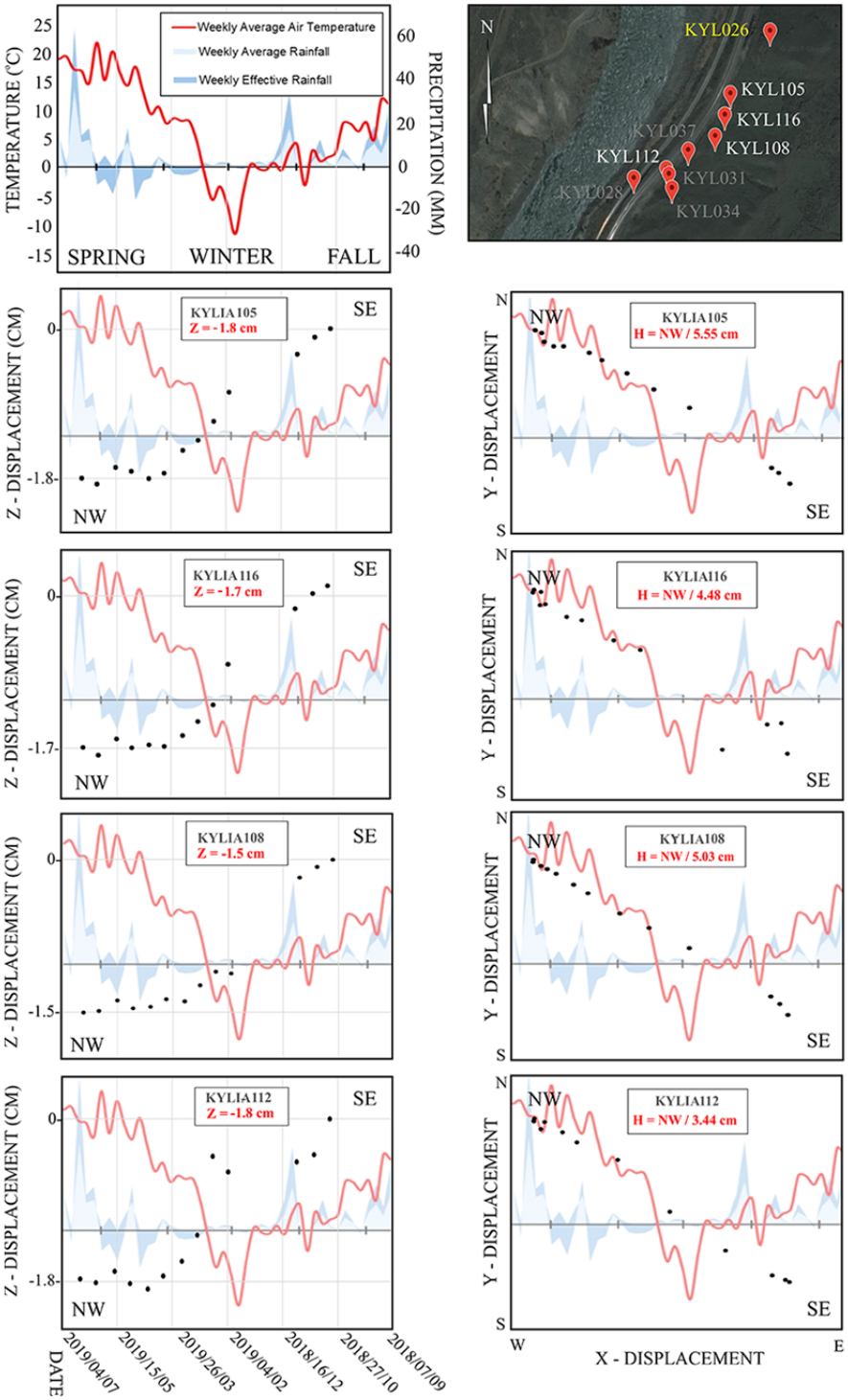

Fig. 9 Geocube™ d-GNSS displacement results: Z - vertical amounts (cm) and X,Y - horizontal displacements trends for the period September 07, 2018 to June 04, 2019; superimposed are rainfall and temperature data from Thomson Valley weather station (Holmes et al. 2020; Huntley et al. 2020a). Note that these graphical representations read right to left to represent the displacement trends across Ripley Landslide.

4.4 UAV surveying and change detection monitoring

Individually, DSMs capture the surface condition of the landslide, including vegetation growth (e.g., grasses, shrubs, and trees) that only partly obscure the bare earth. These conditions are sufficient for surface change detection mapping using successive

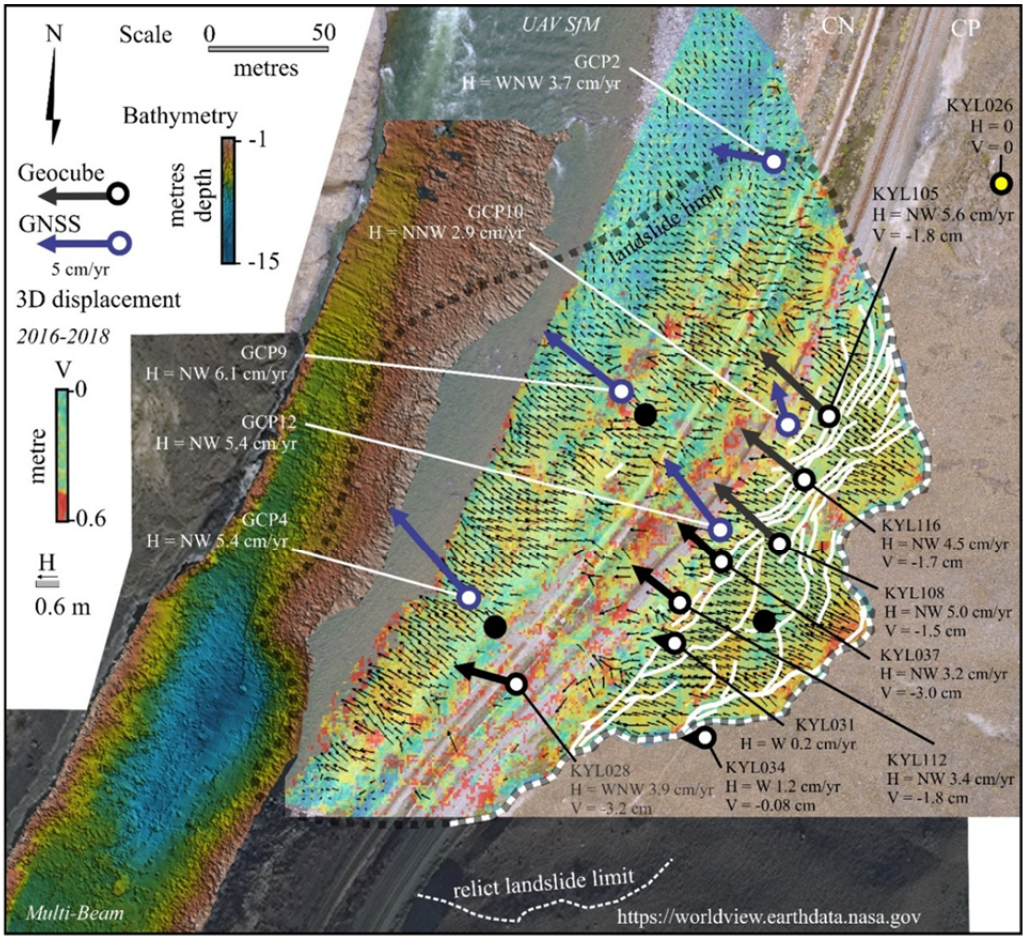

Fig. 10 Surface displacement data derived from UAV overflights in 2016 and 2018 and multi-beam bathymetry data collected in 2018; plotted with RTK-GNSS (average annual rate for 2017, 2018 and 2019) and d-GNSS displacement data (November 2018 to June 2019, expressed as cm/yr). Figure also merges multibeam bathymetry data of Thompson River with an outline of Ripley Landslide mapped from a WorldView-2 image of the study site. Stable d-GNSS unit – yellow dot; active d-GNSS unit – black and white dot; inactive Geocube – black dot. Active GCP - blue dot.

DSMs. Metre-scale features (e.g., boulders, corner reflectors) are identifiable, and NW horizontal and vertical displacements of 20-30 cm, and 15 cm respectively have been measured throughout the slide area on the UAV aerial photography (Fig. 10). Within the slide boundary, an average movement of 23 cm between September 2016 and September 2017 is derived. Adjacent to the landslide, an average difference of 1.64 cm, and up to 4.4 cm is calculated (within the RMS error of the RTK-GNSS, and 3D point cloud processing). Measured flow direction of the landslide material is consistently downslope. The absolute position of the rail tracks has moved between 12 cm and 27 cm, NW.

UAV photogrammetry reveals that the direction of displacement changes across the landslide (Fig. 10). Over much of the slide body movement is to the NW, except along the northern and southern flanks, where displacement is W. In contrast, channel scour along the slide toe, and submerged bedrock bounding the landslide, drives the body mass generally to the W. Cosi-Corr results from 2016-2018 show >50 cm NW displacement of blocks along steep-dipping, retrogressive backscarps to the main slide body (Fig. 10). This high value is consistent with the InSAR and GNSS monument data that captured significant displacement in 2017 (Fig. 3). Displacement along the tracks reflects subsidence of the slide body (also expressed in deformation of the lock-block retaining wall), and the addition of ballast during routine safety maintenance. A zone of high displacement at the south flank of the slide foot is likely the consequence of toe-slope erosion as evidenced by the 15 m-deep scour pool mapped by the bathymetric surveys (Fig. 10). Across much of the foot slope however, 3D displacement values are lower, reflecting translational

movement of the slide mass over sub-horizontal failure planes beneath the tracks and river.

5 Discussion

Understanding the geographic distribution, and temporal range of earth materials and geological hazards, and their potential responses to meteorological extremes are essential for a resilient transportation network; in addition to protecting natural resources, local communities, traditional land-use practices, and the national economy. Monitoring unstable slopes and infrastructure at risk is a cost-effective hazard management practice that also provides important geoscience information to help develop appropriate mitigation and adaptation measures.

5.1 Landslide change detection

At Ripley Landslide, scour pool and cutbank erosion (Fig. 1b; Fig. 2b) are evidence that Thompson River is actively incising the channel floor where bedrock and rock fall debris constricts stream flow and locally increases current velocity. Channel incision and cutbank erosion produce over-steepened toe slopes, and expose deep-seated rupture planes in submerged slide blocks. Seasonal loading and unloading of submerged toe slopes unloading contribute to movement on rupture surfaces (cf. Porter et al. 2002; Eshraghian et al. 2007; Eshraghian et al. 2008). Toe slope incision is occurring adjacent to where the highest ground motion rates are recorded when river and groundwater levels are low (Macciotta et al. 2014; Hendry et al. 2015; Schafer et al. 2015; Journault et al. 2018). This is also where critical railway infrastructure is at the greatest risk (i.e., the lock-block retaining wall and tracks).

The greatest displacement rates detected by the d-GNSS network, InSAR, GNSS monuments, RTK-GNSS surveys, and UAV photogrammetry occur from winter to spring. During these seasons, transitional ground conditions allow snow melt and rainfall to penetrate deep into the still-frozen (or thawing) slide body by way of tension cracks, planar fractures, and bedding surfaces (Holmes et al. 2020; Huntley et al. 2020a). Between late fall (November) and early spring (March), as snowfall blankets the slope, the ground freezes (<0°C) to an estimated depth <2 m. When air temperatures are >0°C, rain and melting snow result in an increase in moisture content of sub-surface clay-rich units (Huntley et al. 2019b; Holmes et al. 2020). That peak displacement is observed through winter to spring, implies that low river and groundwater levels are necessary for significant movement (Fig. 9).

Slope instability is triggered when the river level and groundwater head on landslide rupture surfaces fall after summer peak discharge (cf. Porter et al. 2002; Eshraghian et al. 2007; Eshraghian et al. 2007; Hendry et al. 2015; Schafer et al. 2015). During summer months, Thompson River levels are high and buttress the submerged portions of the toe slope. Groundwater is at its maximum level within the slide body. It is during this period that InSAR techniques and GNSS monuments capture minimum surface displacement (Journault et al. 2018; Huntley et al. 2019c). The d-GNSS network record that the downward displacement trends of winter are interrupted by slight surface rise-and-fall events in late spring (May) to early summer (June). Uplift-subsidence events appear to be responses to antecedent precipitation events and seasonal temperature changes (Fig. 9).

Combining the results of the RTK-GNSS surveys, d-GNSS network, and UAV change detection reveals a detailed map of surface displacement across the slide (Fig. 10). Cosi-Corr results show the greatest horizontal and downward displacement along the headscarp, and individual blocks in the main slide body. Here, transtension and transpression of slide blocks is driven by movement along steep, retrogressing backscarps. Across the slide toe, there is considerably less vertical displacement associated with translational movement along sub-horizontal failure planes beneath the tracks, ballast, lock-block retaining wall and river.

TK-GNSS, d-GNSS units, and UAV photogrammetry reveal that the direction of displacement changes across the landslide (Fig. 10). Upslope of the tracks, displacement is NW across much of the slide body, except along northern and southern flanks where displacement is W. Downslope of the tracks, the slide mass moves W. This change in creep direction is a response to channel scour of the slide toe, and the presence of shallow bedrock confining the north and south flanks of Ripley Landslide.

5.2 Evaluation of GeocubesTM

Together with RTK-GNSS, bathymetric and UAV surveys, d-GNSS Geocube™ spatial data help landslide researchers understand the behaviour and drivers of slope instabilities affecting rail transport in the Thompson River valley. Detailed examination of d-GNSS records provides new insight on the rates and spatial pattern of creep, and also on the timing and possibly precursors of changes in creep behaviour. The spatial variability in landslide motion is a surface expression slope failure involving complex interactions between structurally separate blocks. Comparing displacement trends with temperature, precipitation, river level, and ground resistivity will help establish landslide warning thresholds based on environmental conditions. The locations of highest displacement rates as indicted by the d-GNSS network can be used to identify where track damage will be expected if creep continues across Ripley Landslide.

A number of issues are contributing to lengthy installation and evaluation periods, including wildlife, technical limitations, and environmental concerns. Steep mountainous terrain and vegetation limit visibility of the sky and create multipath effects, decreasing the effectiveness of some d-GNSS units. Several units were damaged by cattle, deer, rodents and other large mammals, requiring innovative methods to protect cables and hardware. Cable damage by wildlife, and lack of battery power prevented the system from functioning throughout parts of 2016 and 2017. Fortunately, other monitoring captured the large displacement event of winter-spring 2017, illustrating the benefit of redundancy with other instrumentation. These issues were addressed between November 2017 and October 2018 with the addition of protective wrappings to cables, through the adjustment of d-GNSS units and solar panel positions, and installation of upgraded batteries and battery boxes.

As an emerging technology, software updates and changes in product designs require frequent re-installation and re-calibration of the d-GNSS network. The Thompson River valley is an extremely harsh environment for electronic systems. Considerable time was spent making hardware more rugged and weatherproof. By November 2018, the d-GNSS network at Ripley Landslide was fully “ruggedized” and linked via remote internet connections to updated data processing software. Moving forward, the research goal will be to develop a d-GNSS monitoring protocol and tools that capture patterns and rates of movement, and changes in landslide activity. Comparing displacement trends with temperature, precipitation, river level, and ground resistivity will help establish landslide warning thresholds based on environmental conditions, and used to forecast pending failures.

6 Summary: Best Practices for Understanding and Monitoring Landslides

This study combines terrain mapping and change detection techniques to understand and monitor a representative slow-moving landslide in the Thompson River valley railway transportation corridor of south-central British Columbia (Fig. 1a, b; Fig. 11). Landslide form, and nature the adjacent stable slopes and water bodies were best described through surficial geology mapping, bathymetric and geophysical surveys, real-time monitoring of movement, groundwater, and geophysical properties in boreholes. Change detection monitoring employing emerging airborne and spaceborne platforms, ground-based GNSS systems, fibre optics, and climate variables best captured landslide function (Fig. 11).

Slopes along the Thompson River valley transportation corridor are susceptible to landslides, floods, and other geohazards triggered by extreme weather events, slope engineering, and agricultural practices. At Ripley Landslide, InSAR, GNSS, and UAV datasets record increased activity and ground displacement from late winter to early spring, reflecting seasonal and spatial variations in precipitation, temperature, river levels, and groundwater recharge in the Thompson River valley. Railway infrastructure (e.g., tracks, ballast, bridges, tunnels, and retaining walls), operational activities, the natural environment, and public safety are all expected to be adversely impacted by future landslides triggered by extreme weather driven by climate change. In the coming years, research and monitoring efforts will aim to gain a better understanding of how extreme weather, climate change, and landslide hazards impact the national railway network. This fundamental geoscience information will help build more robust risk tolerance, remediation, and mitigation strategies to maintain the

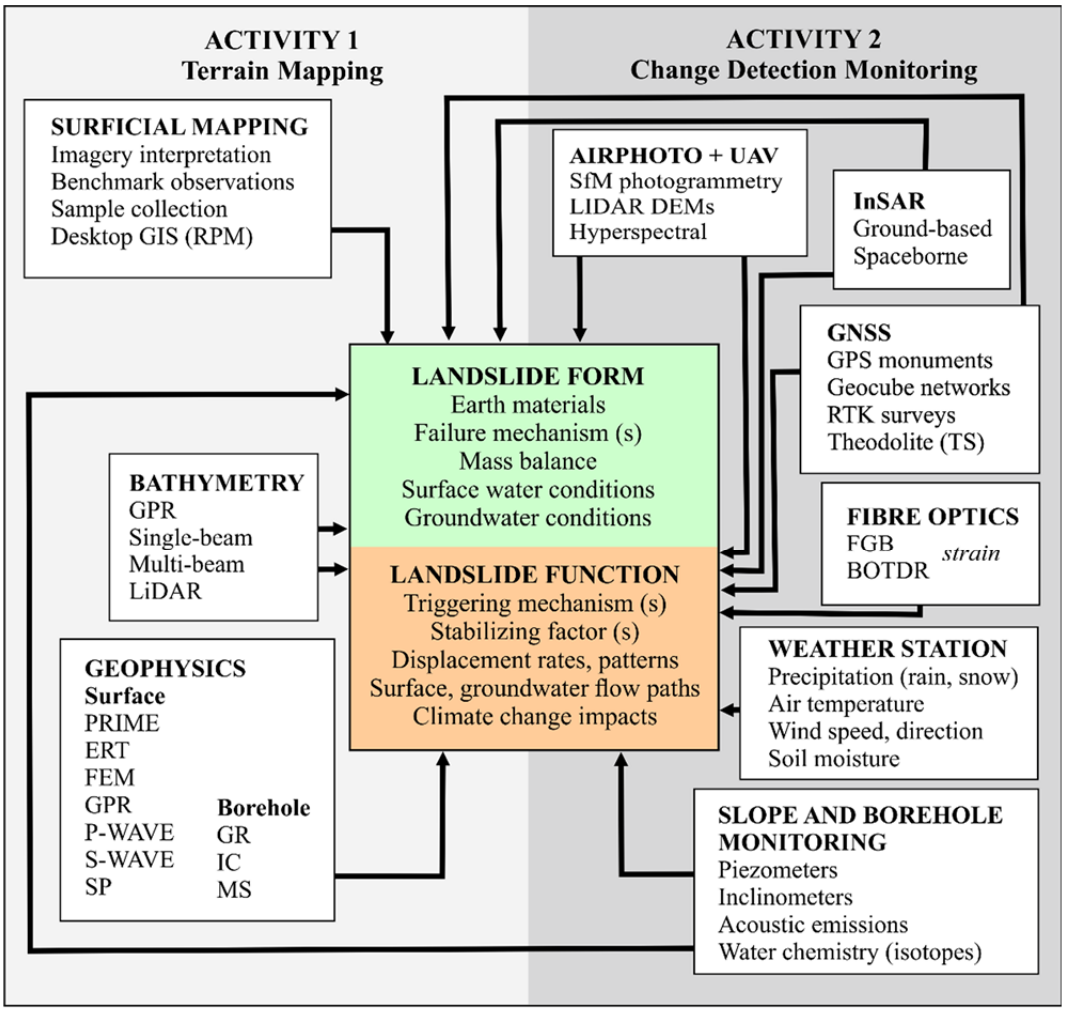

Fig. 11 Best practices for terrain mapping and change detection monitoring of landslide systems, based on experience in the Thompson River valley, British Columbia (2013-2020).

resilience of vulnerable transportation infrastructure along strategically important sections of the national railway network, while also protecting public safety, the natural environment, community stakeholders, and Canadian economy.

Acknowledgments

The Government of Canada - through the Ministry of Transport and Ministry of Natural Resources - funded this research. Fieldwork would not be possible without the support of Trevor Evans (Canadian National Railways, Kamloops, British Columbia), Danny Wong (Canadian Pacific Railways, Calgary, Alberta) and Jason Bojey (Canadian Pacific Railways, Kamloops, British Columbia). University and international partners include Michael Hendry, Renato Macciotta, Jorge Rodriguez, Kevin Wallin, and Evan Deane (University of Alberta, Edmonton, Alberta); David Elwood and Kelvin Sattler (University of Saskatchewan, Saskatoon, Saskatchewan); Shane Donohue (University College Dublin, Ireland) and Jessica Holmes (Queen's University, Belfast, Northern Ireland); Jonathan Chambers, Philip Meldrum and Paul Wilkinson (British Geological Survey, Keyworth, UK). Bathymetric surveys were completed with the assistance of Tim Funk (Funktional, Kamloops, British Columbia), Paul Bauman, Graham Young and team (Advisian-Worley Parsons Group, Calgary, Alberta), and Jacques Gagne (Department of Fisheries and Oceans, Sidney, British Columbia). Andrew Pon and colleagues (3vGeomatics, Vancouver, British Columbia) and Pano Skrivanos (Pacific UAV, Sidney, British Columbia) provided technical assistance with InSAR and UAV analyses.

Remi Usquin and Frédéric Verluise, Ophelia Sensors (Paris, France), provided tireless Geocube ™ support. The authors wish to thank Melanie Kelman (Geological Survey of Canada, Vancouver) for an internal peer review. The final manuscript benefitted from helpful comments by two critical reviewers for the Journal of Mountain Science.

References

Aydin NZ, Duzgun HS, Heinimann HR, et al. (2018) Framework for improving the resilience and recovery of transportation networks under geohazard risks. Int J Disast Risk Re 31: 832-843. https://doi.org/10.1016/j.ijdrr.2018.07.022

Baum R, McKenna J, Godt J, et al. (2005) Hydrologic monitoring of landslide-prone coastal bluffs near Edmonds and Everett, Washington, 2001-2004. USGS Open-File Report 1063. 42 p.

Benoit L, Briole P, Martin O, et al. (2015) Monitoring landslide displacements with Geocube wireless network of low-cost GPS. Eng Geol 195: 111-121. https://doi.org/10.1016/j.enggeo.2015.05.020

Bobrowsky P, Dominguez M (2012) Landslide susceptibility map of Canada. GSC Open File 7228: 1 sheet. https://doi.org/10.4095/291902

Bobrowsky P, Sladen W, Huntley D, et al. (2014) Multi-parameter monitoring of a slow moving landslide: Ripley Slide, British Columbia, Canada. In: Lollino G, et al (eds), Engineering Geology for Society and Territory, Landslide Processes (Volume 2), IAEG Congress, Springer Publishing. pp 155-159.

Bobrowsky P, Huntley D, Neelands P, et al. (2017) Ripley Landslide – Canada's premier landslide field laboratory. In: Abstracts and Proceedings, GSA Annual Meeting. 1 p.

Bobrowsky P, MacLeod R, Huntley D, et al. (2018) Ensuring Resource Transport Safety: Monitoring Critical Infrastructure with UAV Technology. In: Proceedings Volume and Abstracts, Resources for Future Generations. 1 p.

Bunce C, Chadwick I (2012) GPS monitoring of a landslide for railways. In: Eberhardt E, et al. (eds), Landslides and Engineered Slopes - Protecting Society through Improved Understanding. pp 1373-1379.

Doll C, Trinks C, Sedlacek N, et al. (2014) Adapting rail and road networks to weather extremes: case studies for southern Germany and Austria. Nat Haz 72: 63-85. https://doi.org/10.1007/s11069-013-0969-3

Eshraghian A, Martin C, Cruden D (2007) Complex earth slides in the Thompson River Valley, Ashcroft, British Columbia. Environ Eng Geosci 13(2): 161-181 https://doi.org/10.2113/gseegeosci.13.2.161

Eshraghian A, Martin C, Morgenstern N (2008) Movement triggers and mechanisms of two earth slides in the Thompson River Valley, British Columbia, Canada. Can Geotech J 45: 1189-1209. https://doi.org/10.1139/T08-047

Geertsema M, Schwab J, Blais-Stevens A, et al. (2009) Landslides impacting linear infrastructure in west central British Columbia. Nat Haz 48: 59-72 https://doi.org/10.1007/s11069-008-9248-0

Gibson A, Culshaw M, Dashwood C, Pennington C (2013) Landslide management in the UK – the problem of managing hazards in a 'low-risk' environment. Landslides 10: 599-610. https://doi.org/10.1007/s10346-012-0346-4

Gili J, Corominas J, Rius J (2000) Using Global Positioning System techniques in landslide monitoring. Eng Geol 55 (3): 167-192. https://doi.org/10.1016/S0013-7952(99)00127-1

Haque U, Blum P, da Silva P, et al. (2016) Fatal landslides in Europe. Landslides 13: 1545-1554 https://doi.org/10.1007/s10346-016-0689-3

Hendry M, Macciotta R, Martin D (2015) Effect of Thompson River elevation on velocity and instability of Ripley Slide. Can Geotech J 52(3): 257-267. https://doi.org/10.1139/cgj-2013-0364

Holmes J, Chambers J, Meldrum P, et al. (2020) 4-Dimensional Electrical Resistivity Tomography for continuous, near-real time monitoring of a landslide affecting transport infrastructure in British Columbia, Canada. NSG. 15 p. https:// doi.org/10.1002/nsg.12102

Huntley D, Bobrowsky P (2014) Surficial geology and monitoring of the Ripley Slide, near Ashcroft, British Columbia, Canada. GSC Open File 7531. 21 p.

Huntley D, Bobrowsky P, Zhang Q, et al. (2016) Application of Optical Fibre Sensing Real-Time Monitoring Technology at the Ripley Landslide, near Ashcroft, British Columbia, Canada. Can Geotech Soc GeoVancouver 2016. 13 p.

Huntley D, Bobrowsky P, Parry N, et al. (2017a) Ripley Landslide: the geophysical structure of a slow-moving landslide near Ashcroft, British Columbia, Canada. GSC Open File 8062. 59 p.

Huntley D, Bobrowsky P, Best M (2017b) Combining terrestrial and waterborne geophysical surveys to investigate the internal composition and structure of a very slow-moving landslide near Ashcroft, British Columbia, Canada. In: Mikos M, Tiwari B, Yin Y, Sassa K (eds) Advancing Culture of Living with Landslides. WLF 2017. Springer, Cham. pp 179-190. https://doi.org/10.1007/978-3-319-53498-5_21

Huntley D, Bobrowsky P, Charbonneau F, et al. (2017c) Innovative landslide change detection monitoring: application of space-borne InSAR techniques in the Thompson River valley, British Columbia, Canada. In: Mikos M, Tiwari B, Yin Y, Sassa K (eds) Advancing Culture of Living with Landslides. WLF 2017. Springer, Cham. pp 219-229. https://doi.org/10.1007/978-3-319-53487-9_25

Huntley D, Bobrowsky P, Zhang Q, et al. (2017d) Fibre Bragg Grating and Brillouin Optical Time Domain Reflectometry Monitoring Manual for the Ripley Landslide, near Ashcroft, British Columbia. GSC Open File 8258. 66 p.

Huntley D, Bobrowsky P, Hendry M, et al. (2019a) Multi-technique geophysical investigation of a very slow-moving landslide near Ashcroft, British Columbia. Canada. J Environ Eng Geophys 24: 87-110. https://doi.org/10.2113/JEEG24.1.87

Huntley D, Bobrowsky P, Hendry M, et al. (2019b) Application of multi-dimensional electrical resistivity tomography datasets to investigate a very slow-moving landslide near Ashcroft, British Columbia, Canada. Landslides 16: 1033-1042 https://doi.org/10.1007/s10346-019-01147-1

Huntley D, Bobrowsky P, Sattler K, et al. (2019c) PRIME installation in Canada: protecting national railway infrastructure by monitoring moisture in an active landslide near Ashcroft, British Columbia. GSC Open File 8548. 1 poster. https://doi.org/10.4133/sageep.32-063

Huntley D, Holmes J, Bobrowsky P, et al. (2020a) Hydrogeological and geophysical properties of the very slow-moving Ripley Landslide, Thompson River valley, British Columbia. Can J Earth Sci 57(1):1-21. https://doi.org/10.1139/cjes-2019-0187

Huntley D, Bobrowsky P, Cocking R, et al. (2020b) Installation,

operation and evaluation of an innovative global navigation satellite system monitoring technology at Ripley Landslide and South Slide, near Ashcroft, British Columbia. GSC Open File 8742. 36 p.
https://doi.org/10.4095/327125

Jaiswal P, van Westen C, Jetten V (2010) Quantitative assessment of direct and indirect landslide risk along transportation lines in southern India. Nat Haz Earth Syst Sci 10: 1253-1267.

Jespersen-Groth J, Potthoff D, Clausen J, et al. (2009) Disruption management in passenger railway transportation. In: Robust and Online Large-Scale Optimization. Springer, Berlin, Heidelberg. pp 399-421.
https://doi.org/10.1007/978-3-642-05465-5_18

Journault J, Macciotta R, Hendry M, et al. (2018) Measuring displacements of the Thompson River valley landslides, south of Ashcroft, B.C., Canada, using satellite InSAR. Landslides 15: 621-636.
https://doi.org/10.1007/s10346-017-0900-1

Ko Ko C, Chowdhury R, Flentje P (2005). Hazard and risk assessment of rainfall-induced landsliding along a railway line. Q J Eng Geol Hydroge 38: 197-213.
https://doi.org/10.1144/1470-9236/04-004

Laimer H (2017) Anthropogenically-induced landslides – a challenge for railway infrastructure in mountainous regions. Eng Geol 222: 92-101.
https://doi.org/10.1016/j.enggeo.2017.03.015

Lindgren J, Jonsson D, Carlsson-Kanyama A (2009) Climate adaptation of railways: lessons from Sweden. Eur J Transp Infrastruct Res 9 (2): 164-181

Macciotta R, Hendry M, Martin D, et al. (2014) Monitoring of the Ripley Slide in the Thompson River Valley, B.C. In: Proceedings and Abstracts Volume, Geohazards 6 Symposium. 1 p.

Macciotta R, Hendry M, Rodriguez J, et al. (2017) The 10-Mile Slide north of Lillooet, British Columbia – history, characteristics and monitoring. In: 3rd North American Symposium on Landslides, AEEG. pp 937-948.

Malet JP, Maquaire O, Calais E (2002) The use of Global Positioning System techniques for the continuous monitoring of landslides: application to the Super-Sauze earthflow (Alpes-de-Haute-Provence, France). Geomorphology 43 (1-2): 33-54.
https://doi.org/10.1016/S0169-555X(01)00098-8

Martinović K, Gavin K, Reale C (2016) Development of a landslide susceptibility assessment for a rail network. Eng Geol 215: 1-9.
https://doi.org/10.1016/j.enggeo.2016.10.011Get rights and content

Newman P, Kenworthy J, Glazebrook G (2013) Peak care use and rise of global rial: why is this happening and what it means for large and small cities. J Transport Tech 3 (4): 16 p.

Petrova E (2011) Critical infrastructure in Russia: geographical analysis of accidents triggered by natural hazards. Environ Eng Manage J 10 (1): 53-38.

Porter M, Savigny K, Keegan T, et al. (2002) Controls on stability of the Thompson River landslides. In: Proceedings of the 55th Canadian Geotechnical Conference: Ground and Water – Theory to Practice. Can Geotech Soc. pp 1393-1400.

Renner M, Gardner G (2010) Global competitiveness in the rail and transit industry. Worldwatch Institute. 30 p.

Rodriguez J, Hendry M, Macciotta R, Evans T (2018) Cost-effective Landslide Monitoring GPS: Characteristics, Implementation and Results. In: Geohazards. Canmore, Canada. 8 p.

Ronchetti F, Borgatti L, Cervi F, et al. (2009) Groundwater processes in a complex landslide, northern Apennines, Italy. Nat Haz Earth Syst Sci 9: 895-904.
https://doi.org/10.1080/17445647.2020.1837270

Raso E, Brandolini P, Faccini F, et al. (2017) Geomorphological evolution and monitoring of San Bernadino-Guvano coastal landslide (eastern Ligurai, Italy). Geog Fisk Dina Quat 40: 197-210.
https://doi.org/10.1080/17445647.2020.1837270

Sa'adin S, Kaewunruen S, Jaroszweski D (2016) Risks of climate change with respect to the Singapore-Malaysia high speed rail system. Climate 4 (4): 65.
https://doi.org/10.3390/cli4040065

Schafer M, Macciotta R, Hendry M, et al. (2015) Instrumenting and Monitoring a Slow Moving Landslide. In: GeoQuebec 2015 – Challenges from North to South. Québec . 7 p.

Schuster R, Fleming R (1986) Economic losses and fatalities due to landslides. Bull Assoc Eng Geol XXIII (1): 11-28.
https://doi.org/10.2113/gseegeosci.xxiii.1.11

Skrucany T, Kendra M, Skorupa M, et al. (2017) Comparison of chosen environmental aspects in individual road transport and railway passenger transport. Proc Eng 192: 806-811.
https://doi.org/10.1016/j.proeng.2017.06.139

Stanton RB (1898) The great land-slides on the Canadian Pacific Railway in British Columbia. Proc Civil Eng 132(2): 1–48.
https://doi.org/10.1680/imotp.1898.19167

Sun S, Wang J, Zheng J (2013) Analysis of a railway embankment landslide induced by the Wenchuan Earthquake, China. Soil Mech Found 15 (2): 56-60.
https://doi.org/10.1007/s11204-013-9210-3

VanDine D (1983) Drynoch landslide, British Columbia – a history. Can Geotech J 20 (1): 82-103.
https://doi.org/10.1139/t83-009

Yang H, Dijst M, Witte P, et al. (2019) Comparing passenger flow and time schedule data to analyze high-speed railways and urban networks in China. Urban Stud 56 (6): 1267-1287.
https://doi.org/10.1177/0042098018761498